doi:10.1017/S1431927618004099
Microsc. Microanal. 24 (Suppl 1), 2018

The Maia Detector Journey: Development, Capabilities and Applications

C G Ryan[1], D P Siddons[2], R Kirkham[1], A J Kuczewski[2], P A Dunn[1], G De Geronimo[2], A. Dragone[2], Z Y Li[2], G F Moorhead[1], M Jensen[1], D J Paterson[3], M D de Jonge[3], D L Howard[3], R Dodanwela[1], G A Carini[2], R Beuttenmuller[2], D Pinelli[2], L Fisher[1], R M Hough[1], A Pagès[1], S A James[3] and P Davey[1]

[1] CSIRO Mineral Resources, Gate 5 Normanby Rd., Clayton VIC 3168, Australia
[2] Brookhaven National Laboratory, Brookhaven, Upton NY, USA
[3] Australian Synchrotron, Blackburn Road, Clayton VIC 3168, Australia

The development of the Maia detector was motivated by the desire for high throughput synchrotron fluorescence element mapping with images beyond 100 M pixels, which capture both fine detail and extended spatial context. It achieves this by using a large planar silicon detector array together with event-mode data acquisition, where each detected X-ray event is tagged with position in the scan, thus avoiding the readout overheads of a "step and acquire" style of mapping. The sample stage moves continuously and the stage encoders are read by the FPGA based real-time processor to provide coordinates for each event, which provides great freedom in scan speed or transit time per map pixel [1]. The large detector array, with 384 independent detector channels, each with its own charge amplification and pulse capture electronics, implemented using custom ASICs, enables cumulative count-rates exceeding 10 M/s to be achieved with low pile-up probability, which enables adequate counting statistics to be acquired per pixel in transit times as short as 50 µs [2,3]. The array uses a back-scatter, annular configuration, which combines a 1.3 sr solid-angle detection geometry with complete freedom in sample size and scanning range. This has enabled applications to extend from the initial focus on synchrotron X-ray microanalysis, with µm sized pixels and scan ranges up to a few centimeters, to macro-scale mapping using synchrotron or laboratory X-ray sources, with scan ranges up to ~1 m.

The Maia concept was introduced at M&M 2005 and prototypes demonstrated performance using a 32 channel array at the NSLS synchrotron in 2006 [4] and a 96 channel array at the NSLS and Australian Synchrotron (AS) in 2008 [5,6]. The 96-channel prototype demonstrated imaging up to 77 M pixels and transit times as short as 50 µs and demonstrated real-time spectral deconvolution for quantitative imaging using the Dynamic Analysis algorithm implemented in the FPGA [5]. An annular 384 channel Maia detector was commissioned for the XFM beamline of the AS [2,3] and from 2011 it has demonstrated imaging beyond 100 M pixels (largest image 1 G pixels; Fig. 1) with more than 10^5 images and ~100 TB of event data acquired. Now two Maia 384 detectors are in routine application at the XFM beamline [7], one for µm-scale mapping and one for macro-scale mapping of cultural heritage objects. Maia 384 detectors are also in use for SXRF element mapping at the P06 beamline, Petra III synchrotron, DESY in Hamburg [8], the SRX beamline, NSLS-II in New York and the CHESS synchrotron at Cornell University. The large solid-angle and collection efficiency of the Maia 384 detector has been exploited in a pair of laboratory XRF mapping systems called Maia Mapper at CSIRO for high definition element mapping of rock samples and drill core at 30 µm spatial resolution over spatial scales up to 500 mm [9].

Synchrotron XRF mapping using Maia has been applied to studies in the earth, planetary, environmental, medical, biological, chemical and material sciences as well as cultural heritage (see refs cited in [1]). Methods and quantitative imaging techniques developed for Maia, which exploit event acquisition tagged by two or three axis coordinates, include large area, high definition, high throughput

mapping of complex samples [1] (Fig. 1), depth contrast mapping and particle depth determination [10], 3D fluorescence tomography [11], XANES image stacks [12] and XANES slice tomography and quick XANES mapping where beam energy may be the fast axis [13] [14].

[1] C G Ryan *et al*., Journal of Physics: Conference Series 499 (2014) 012002.
[2] R Kirkham *et al*., AIP Conference series 1234 (2010) 240-243.
[3] D P Siddons *et al*., Journal of Physics: Conference Series 499 (2014) 012001.
[4] D P Siddons *et al*., 2006 IEEE Medical Imaging Conf. 2, 4179111, (2007) 725.
[5] C G Ryan *et al.,* AIP Conference Proc. 1221 (2010) 9.
[6] C G Ryan *et al*., Nucl. Instr. Meth A 619 (2010) 37.
[7] D Paterson *et al*., AIP Conf. Proc. 1365 (2011) 219.
[8] U Boesenberg *et al.*, J. Synchrotron Rad. 23 (2016) 1550.
[9] C G Ryan *et al*., J. Instrumentation, in press.
[10] C G Ryan *et al.,* Proc. SPIE 8851, X-Ray Nanoimaging (2014) 88510Q.
[11] E Lombi *et al*., Analytical and Bioanalytical Chemistry 400 (2011) 1637.
[12] B Etschmann *et al.*, Environmental Chemistry 11 (2014) 341.
[13] U Boesenberg *et al.*, J. Synchrotron Rad., in press.
[14] Work performed at the XFM beamline of the Australian Synchrotron and supported by the CSIRO Science and Industry Endowment Fund.

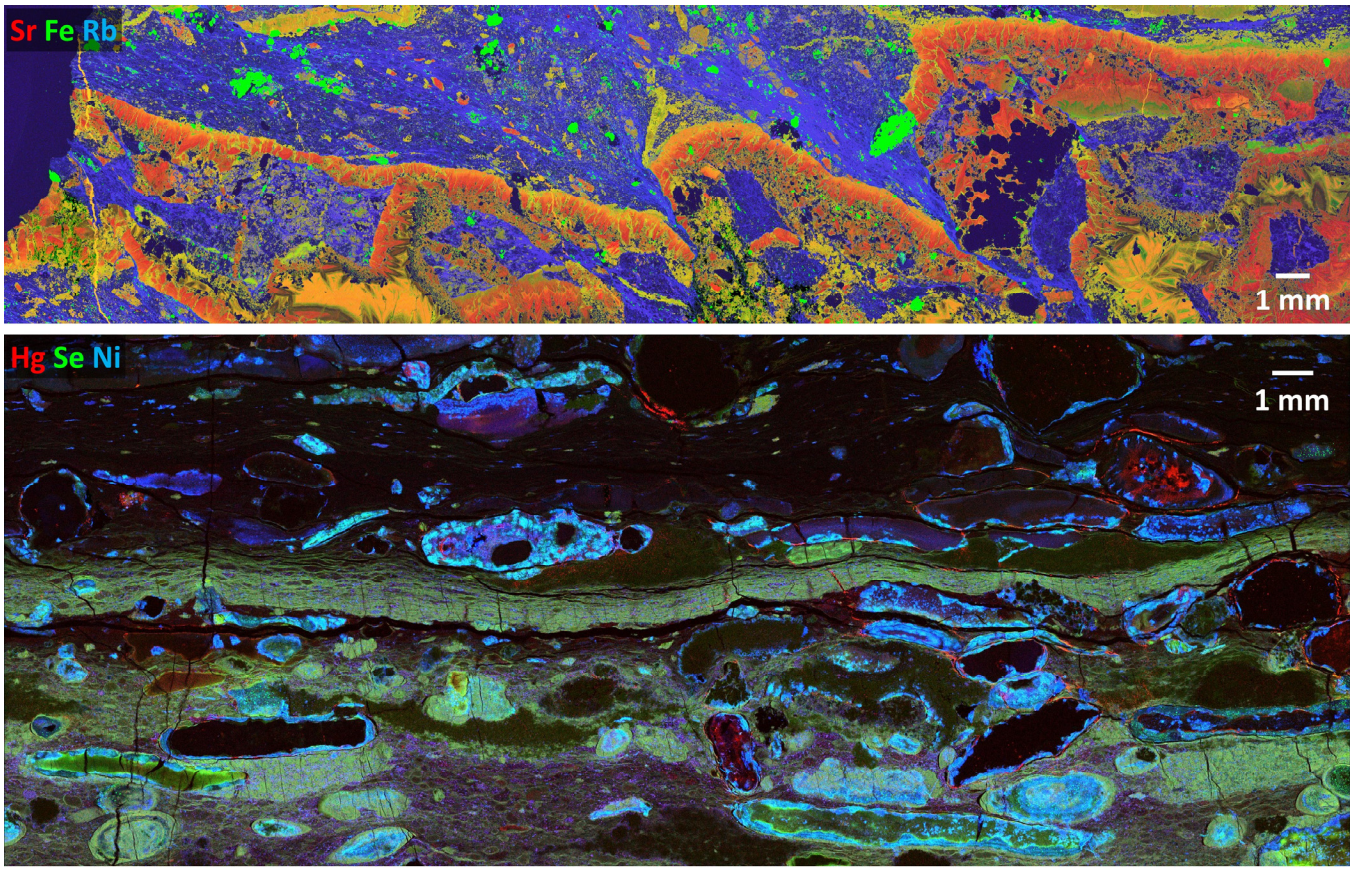

Figure 1. XFM Maia images (18.5 keV X-rays) of samples from the a) Sunrise Dam Gold Mine (Sr, Fe and Rb in RGB, 66668 x 15001 pixels, 40.0 x 9.0 mm^2, 0.13 ms/pixel, 1G pixels), b) Nick metalliferous shale (Hg, Se and Ni in RGB, 8276 x 4526 pixels, 33.1 x 18.1 mm^2, 0.67 ms/pixel, 37M pixels).

https://doi.org/10.1017/S1431927618004099 Published online by Cambridge University Press